



Thermoelectric properties of Coulomb-blockaded fractional quantum Hall islands

Lachezar S. Georgiev

Institute for Nuclear Research and Nuclear Energy, Bulgarian Academy of Sciences, 72 Tsarigradsko Chaussee, 1784 Sofia, Bulgaria

Received 15 January 2015; received in revised form 18 February 2015

Available online 13 March 2015

Editor: Hubert Saleur

Abstract

We show that it is possible and rather efficient to compute at non-zero temperature the thermoelectric characteristics of Coulomb blockaded fractional quantum Hall islands, formed by two quantum point contacts inside of a Fabry–Pérot interferometer, using the conformal field theory partition functions for the chiral edge excitations. The oscillations of the thermopower with the variation of the gate voltage as well as the corresponding figure-of-merit and power factors, provide finer spectroscopic tools which are sensitive to the neutral multiplicities in the partition functions and could be used to distinguish experimentally between different universality classes sharing the same electric properties. We also propose a procedure for measuring the ratio $r = v_n/v_c$ of the Fermi velocities of the neutral and charged edge modes for filling factor $\nu_H = 5/2$ from the power-factor data in the low-temperature limit.

© 2015 The Author. Published by Elsevier B.V. This is an open access article under the CC BY license (<http://creativecommons.org/licenses/by/4.0/>). Funded by SCOAP³.

1. Introduction

Investigating the thermoelectric properties of strongly correlated two-dimensional electron systems is expected to reveal important information about the structure of the neutral excitations [1] and other specific characteristics of their universality classes. Distinguishing between different candidate states describing fractional quantum Hall (FQH) universality classes is interesting because some of them are expected to have particle-like excitations obeying non-Abelian

E-mail address: lgeorg@inrne.bas.bg.

exchange (or braid) statistics [2–4]. Besides the fundamental importance of non-Abelian quasiparticles as new types of particles with exotic statistics, which could only exist in two dimensions, they are also believed to play a crucial role in the field of topological quantum computation where the strange but very robust braid statistics of the quasiparticles in combination with the topology of the quantum registers could efficiently protect quantum information against noise and decoherence [5,6].

In an attempt to distinguish between the different candidates for the $\nu = 5/2$ FQH state, people have investigated the Coulomb-blockade (CB) conductance patterns of FQH islands in states from different universality classes, including at non-zero temperature [7–10]. Unfortunately the CB data appears to be insufficient at low temperature [11] for distinguishing different states because FQH states from different universality classes have been shown to have identical CB conductance peak patterns at zero temperature.

Recently, an emerging possibility to detect non-Abelian statistics by measuring the thermoelectric properties of different FQH states in the CB regime of a Fabry–Pérot interferometer [1] has attracted some attention. The thermoelectric conductance of candidate FQH states at filling factors $\nu_H = 2/3$ and $\nu_H = 5/2$ in a CB island have been computed [1] from the conformal field theory (CFT) data of the underlying effective field theories for the edge excitations. It has been demonstrated that thermoelectric conductance of the quantum dot formed inside of the Fabry–Pérot interferometer might be sensitive to the neutral degrees of freedom of the FQH states expressed in eventually measurable asymmetries for even number of localized quasiparticles in the bulk. However, it appeared that the computation of the thermoelectric conductance for $\nu_H = 5/2$ strongly depends on the ratio $r = v_n/v_c$ of the Fermi velocities of the neutral and charged edge modes, which has to be considered as a free parameter. In Ref. [1] the value $r \approx 1/6$ has been chosen with the argument that it is consistent with previous numerical and experimental work.

Another thermoelectric quantity, the thermopower, known also as the Seebeck coefficient, has been previously computed for metallic quantum dots [12,13] indicating to be a better spectroscopic tool than the transport coefficients alone, while showing the same periodicity as the CB conductance peaks. So far, the computations of thermopower for CB islands in quantum Hall states have been limited to the case of integer ν_H where it is similar to that of the metallic islands. Recently, the thermopower for the $\nu_H = 1/m$ Laughlin FQH states has been computed [14] showing that it is similar to the integer quantum Hall states, except that the oscillation period in the dimensionless Aharonov–Bohm flux (related to the gate voltage) is extended from 1 to m .

The chiral edge excitations determining the topological order of the FQH universality classes have been successfully described by CFTs [15–18]. In this paper we will show how to use the CFT partition function for a general chiral FQH state, as a thermodynamic potential for the experimental setup of Refs. [10,1], in order to calculate the thermopower for a CB island, or a quantum dot (QD), at non-zero temperature. Measuring the power factor computed from the thermopower could experimentally help us to estimate the ratio $r = v_n/v_c$ of the Fermi velocities of the neutral and charged edge modes and eventually to distinguish between the different $\nu_H = 5/2$ states.

The rest of this paper is organized as follows: in Section 2 we explain how the thermopower of a Coulomb blockaded fractional quantum Hall island can be expressed in terms of the Grand-canonical averages of the edge states' Hamiltonian and particle number operators. In Section 3 we review the structure of the Grand-canonical partition functions for general FQH states on a disk and discuss how they are modified in presence of Aharonov–Bohm flux. In Section 4 we

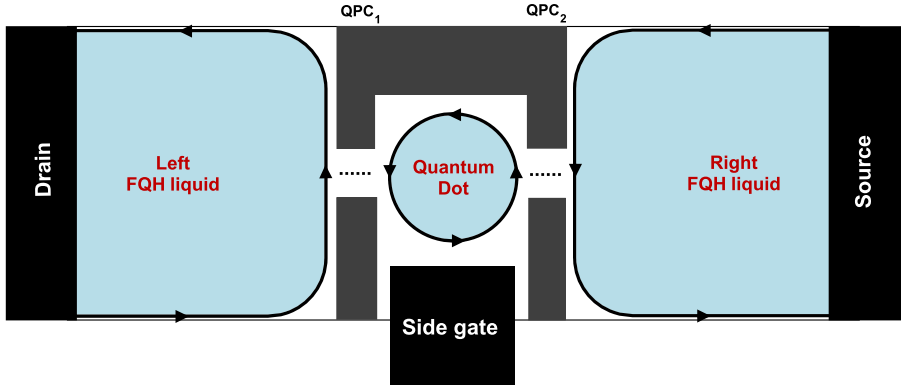


Fig. 1. Single-electron transistor realized by two quantum-point contacts (QPC₁ and QPC₂) inside of a FQH bar. The arrows show the direction of the propagation of the edge modes. Only electrons can tunnel between the left and right FQH liquids and the QD under appropriate conditions and the dots mark the electron tunneling paths.

consider as an example the proposed paired states, the Pfaffian state, the Halperin 331 state, the $SU(2)_2$ and the anti-Pfaffian state, which are candidates to describe the universality class of the fractional quantum Hall state at filling factor $\nu_H = 5/2$. We calculate numerically and plot the thermopower, the electric and thermal conductances and the power factors for these states with odd or even number of bulk quasiparticles. We finish by a discussion of the open problems related to the description of FQH states with counter-propagating modes and give some additional information in three appendices.

2. Thermopower as average tunneling energy of FQH edge excitations

The thermopower is defined [12] as the potential difference V between the left and right leads of the single-electron transistor (SET), formed by the CB island (or QD) and the Drain, Source and Side gate as shown in Fig. 1, when their temperature differs by $\Delta T = T_R - T_L \ll T_L$, under the condition that the electric current I is 0. It is usually computed [12] as the ratio

$$S = \frac{G_T}{G} \tag{1}$$

of the thermal and electric conductances, G_T and G respectively, however, it can be alternatively expressed in terms of the average energy $\langle \varepsilon \rangle$ of the electrons tunneling through the Coulomb-blockaded quantum dot [12]

$$S \equiv - \lim_{\Delta T \rightarrow 0} \frac{V}{\Delta T} \Big|_{I=0} = - \frac{\langle \varepsilon \rangle}{eT}, \tag{2}$$

where e is the electron charge and T is the temperature of the CB island. The thermopower is measured in units $V.K^{-1}$ or, as obvious from the right-hand side of Eq. (2), in units $J/(A.s.K)$ in the SI system. Because the electric conductance G is measured in units e^2/h and the thermal conductance G_T is measured in units ek_B/h it follows from Eq. (1) that thermopower can be also measured in units k_B/e . The alternative approach based on the right-hand side of Eq. (2) is more suitable for disconnected systems, such as the SET shown in Fig. 1, because the conductances G_T and G are both zero in large intervals called CB valleys [12], so it is not appropriate to put G in the denominator of (2), while the voltage V is non-zero and can be measured experimentally [19].

The knowledge of the thermopower and the conductances allow us to compute another important thermoelectric characteristics [20]—the thermoelectric figure-of-merit

$$ZT = \frac{S^2GT}{G_T} \quad (3)$$

for the CB island as a quantum dot and the corresponding power factor \mathcal{P}_T , which is defined in terms of the electric power P generated by ΔT as

$$P = V^2/R = \mathcal{P}_T(\Delta T)^2, \quad \mathcal{P}_T = S^2G, \quad (4)$$

where $R = 1/G$ is the electric resistance of the CB island. We emphasize here that Eq. (1) is relevant only when the electric conductance G is non-zero, while the standard formulas for the figure-of-merit (3) and the power-factor (4) are still expressible in terms of the thermopower S even when the ratio (1) is experimentally indeterminate. That is why thermopower carries more information about the strongly interacting electron system than the electric and thermal conductances together.

The power factor \mathcal{P}_T seems to be measurable directly by applying an AC voltage of frequency $f_0/2$, to the side gate, while measuring the thermoelectric current at frequency f_0 [21]. It is worth stressing that the sharp zeros of the power factor \mathcal{P}_T , at very low temperatures, mark precisely the positions of the maximum of the CB conductance peaks and could be used to determine experimentally the ratio $r = v_n/v_c$ of the Fermi velocities v_n and v_c for the neutral and charged modes respectively, see Eq. (29) below. On the other hand the ratio of the two maxima of the power factor \mathcal{P}_T around each CB peak, just like the ratio of the two extrema of G_T in [1], appears to be rather sensitive to the presence of neutral degeneracies in the edge modes due to finite-temperature asymmetries in the conductance peaks [10]. Moreover, it has been shown that \mathcal{P}_T and S could be significantly enhanced in the single-electron-transistor setup due to the Coulomb blockade [22]. Therefore, \mathcal{P}_T and S could eventually be used to distinguish between different FQH universality classes having the same CB peak pattern [11].

In the rest of this section we will describe how to use the CFT for the edge excitations of a disk FQH sample to compute thermopower and power factors of the corresponding CB islands, which is a central result in this paper. To this end, we first identify the average electron tunneling energy in Eq. (2) as the difference between the total energy of the QD with $N + 1$ and N electrons, which have the same bulk but different edge contributions, then we calculate the edge QD energy and edge electron number, in presence of Aharonov–Bohm flux or gate voltage, as the Grand-canonical averages of the twisted CFT Hamiltonian and Luttinger liquid particle number operator, respectively and finally we express these thermal averages in terms of the Grand canonical disk partition function derived within the framework of the CFT for the edge states.

For large CB islands, the total energy of E_{QD} of the QD with N electrons is defined within the *Constant Interaction model* [23] as¹

$$E_{\text{QD}}^{\beta, \mu_N}(\phi) = \sum_{i=1}^{N_0} E_i(B) + \langle H_{\text{CFT}}(\phi) \rangle_{\beta, \mu_N}, \quad (5)$$

where N_0 is the number of electrons in the bulk of the QD and $N - N_0 = N_{\text{el}}$ is the number of electrons on the edge, $E_i(B)$, $i = 1, \dots, N_0$, are the energies of the occupied single-electron

¹ Following Ref. [1] we disregard the electrostatic energy $e^2N^2/2C$ which is subleading for the large CB islands that are of experimental interest.

states in the bulk of the QD. Since we intend to use the CFT partition function of the CB island as a Grand potential the average $\langle \dots \rangle_{\beta, \mu}$ is taken within the Grand canonical ensemble for the FQH edge at inverse temperature $\beta = (k_B T)^{-1}$ and chemical potential μ and $\langle H_{\text{CFT}} \rangle_{\beta, \mu}$ is the Grand canonical average of the Hamiltonian on the edge. At low temperature the number of electrons on the QD is quantized to be integer and the chemical potential of the QD with N electrons is denoted by μ_N .

We will be interested in the sequential tunneling regime [12,10], when the electrons in the SET tunnel through the QD one by one as the gate voltage is varied, which is the dominating mechanism at low temperature for small conductances between the CB island and the “leads”, like in [12,10]. The leads are assumed to be large FQH liquids with energy spacing much smaller than the energy spacing $\Delta\varepsilon$ of the CB island. In this case, within the linear response approximation for low temperature differences ΔT , the average energy of the electrons tunneling through the CB island could be computed as the difference between the average total energy of the QD with $N + 1$ electrons and that for N electrons in presence of AB flux ϕ (or, equivalently, normalized gate voltage)

$$\langle \varepsilon \rangle_{\beta, \mu_N}^{\phi} = \frac{\langle H_{\text{CFT}}(\phi) \rangle_{\beta, \mu_{N+1}} - \langle H_{\text{CFT}}(\phi) \rangle_{\beta, \mu_N}}{\langle N_{\text{el}}(\phi) \rangle_{\beta, \mu_{N+1}} - \langle N_{\text{el}}(\phi) \rangle_{\beta, \mu_N}}. \quad (6)$$

The variation of the side-gate voltage V_g induces (continuously varying) “external charge” $eN_g = C_g V_g$ on the edge [23,24], which is equivalent to the AB flux-induced variation of the particle number $N_{\phi} = \nu_H \phi$, so that we can use instead the AB flux ϕ determined from $C_g V_g / e \equiv \nu_H \phi$ with $\phi = (e/h)(BA - B_0 A_0)$, where A_0 is the area of the CB island and B_0 is the magnetic field at $V_g = 0$. Using the AB flux ϕ instead of the gate voltage is convenient because ϕ can be interpreted mathematically as a continuous twisting of the $\widehat{u}(1)$ charge of the underlying chiral algebra [25,26], which is technically similar to the rational (orbifold) twisting of the $\widehat{u}(1)$ current [27]. All averages entering Eq. (6) could be identified with some derivatives of the thermodynamical Grand potential. The Grand potential $\Omega(\beta, \mu) = -\beta^{-1} \ln Z(\beta, \mu)$, for the FQH edge states, is defined as usual [28] in terms of the Grand canonical partition function

$$Z(\beta, \mu) = \text{tr}_{\mathcal{H}} e^{-\beta(H_{\text{CFT}} - \mu N_{\text{el}})}, \quad (7)$$

where $H_{\text{CFT}} = \Delta\varepsilon(L_0 - c/24)$ is the Hamiltonian for the edge states expressed in terms of the zero mode L_0 of the Virasoro stress tensor [26] (with central charge c). The Luttinger liquid particle number operator $N_{\text{el}} = -\sqrt{\nu_H} J_0$ is expressed in terms of the zero mode J_0 of the normalized $\widehat{u}(1)$ current and $\Delta\varepsilon = \hbar 2\pi \nu_c / L$ is the non-interacting energy spacing in the QD. The Hilbert space \mathcal{H} of the FQH edge states, over which the trace is taken, depends on the type and number of the localized FQH quasiparticles in the bulk.

When the magnetic field B or the area A or the gate voltage V_g are changed from their initial values, B_0 , or A_0 respectively, the partition function $Z(\beta, \mu) = Z(\tau, \zeta)$ is modified by shifting the modular parameters, as proven in [25] (see Eq. (34))

$$\zeta \rightarrow \zeta + \phi\tau, \quad \phi = \frac{C_g}{e\nu_H} V_g, \quad (8)$$

where the modular parameters τ and ζ , used to construct (rational) CFT partition functions [26], are related to the temperature T and chemical potential μ by $\tau = i\pi T_0 / T$, $T_0 = \hbar \nu_c / \pi k_B L$, $\zeta = (\mu / \Delta\varepsilon)\tau$. To understand Eq. (8) physically we recall the Aharonov–Bohm relation: the electron field operator $\psi_{\text{el}}(z)$, where $z = e^{i\varphi}$ is the electron coordinate on the edge circle, is modified in presence of AB vector potential \mathbf{A} as $\psi_{\text{el}}^{\mathbf{A}}(z) = z^{-\phi} \psi_{\text{el}}(z)$, where ϕ is the dimensionless AB

flux (see Eq. (26) in [25]). The AB flux changes the boundary conditions of all charged particles operators and the adiabatic variation of the flux changes the Hilbert space of the edge excitations by a well known procedure called *twisting* in the conformal field theory [26,27,25]. In particular, the partition function (7) changes as [25]

$$Z_\phi(\beta, \mu) = \text{tr}_{\mathcal{H}} e^{-\beta(H_{\text{CFT}}(\phi) - \mu N_{\text{imb}})}, \quad (9)$$

where \mathcal{H} is the untwisted Hilbert space, corresponding to $\phi = 0$, the thermodynamic parameters β and μ are independent of ϕ , and all flux dependence is moved to the twisted operators of energy $H_{\text{CFT}}(\phi)$ and charge imbalance [24] N_{imb} (cf. Eqs. (32) and (33) in [25])

$$H_{\text{CFT}}(\phi) = H_{\text{CFT}} - \Delta\varepsilon\phi N_{\text{el}} + \frac{\nu_H}{2} \Delta\varepsilon\phi^2, \quad N_{\text{imb}} = N_{\text{el}} - \nu_H\phi. \quad (10)$$

The ultimate effect of the AB flux on the partition function $Z(\beta, \mu)$ is shifting ζ as in (8) or, equivalently, $\mu \rightarrow \mu + \phi\Delta\varepsilon$.

It follows from (9) that $\partial\Omega/\partial\mu = -\langle N_{\text{imb}} \rangle_{\beta, \mu}$ and taking into account (10) we find that the thermodynamic average of the electron number in presence of AB flux (setting $\mu = 0$) is

$$\langle N_{\text{el}}(\phi) \rangle_{\beta, \mu} = -\frac{\partial\Omega_\phi(T, \mu)}{\partial\mu} + \nu_H\phi, \quad (11)$$

where $\Omega_\phi(T, \mu) = -k_B T \ln Z_\phi(\beta, \mu)$. This general construction of the electron number operator average in presence of AB flux allows us to compute also the flux dependence of the conductance of the Coulomb island according to Eq. (10) in [10] and Eq. (11) at $\mu = 0$, i.e.,

$$G(\phi) = \frac{e^2}{h} \left(\nu_H + \frac{1}{2\pi^2} \left(\frac{T}{T_0} \right) \frac{\partial^2}{\partial\phi^2} \ln Z_\phi(T, 0) \right). \quad (12)$$

The electron number (11) and the conductance (12) are illustrated for the Pfaffian FQH state in Fig. 5 below. Next, we can compute the average quantum dot energies with N electrons on the edge at temperature T and chemical potential μ in presence of AB flux from the standard Grand canonical ensemble relation [28]

$$\langle H_{\text{CFT}}(\phi) \rangle_{\beta, \mu} = \Omega_\phi(\beta, \mu) - T \frac{\partial\Omega_\phi(\beta, \mu)}{\partial T} - \mu \frac{\partial\Omega_\phi(\beta, \mu)}{\partial\mu}. \quad (13)$$

To summarize the main result in this paper: substituting Eq. (13) and (11) into Eq. (6) we can compute the thermopower of a CB FQH island in terms of the edge state's partition function (9) in presence of Aharonov–Bohm flux or side-gate voltage introduced into the latter through Eq. (8).

3. Thermopower for general FQH disks

The Grand canonical partition function (7) for a general FQH edge states on a disk can be written as [29–31,9]

$$Z^{l, \Lambda}(\tau, \zeta) = \sum_{s=0}^{n_H-1} K_{l+s d_H}(\tau, n_H\zeta; n_H d_H) \text{ch}_{\omega^s * \Lambda}(\tau'), \quad (14)$$

where n_H and d_H are the numerator and denominator of the filling factor $\nu_H = n_H/d_H$ while ω is the neutral topological charge of the electron operator, which is always non-trivial [25] when

$n_H > 1$. The $\widehat{u(1)}$ partition function $K_l(\tau, \zeta; m)$ for the charged part is completely determined by the filling factor ν_H and coincides with that for a chiral Luttinger liquid with a compactification radius [29] $R_c = 1/m$, in the notation of [26,25]

$$K_l(\tau, \zeta; m) = \frac{\text{CZ}}{\eta(\tau)} \sum_{n=-\infty}^{\infty} q^{\frac{m}{2}(n+\frac{l}{m})^2} e^{2\pi i \zeta (n+\frac{l}{m})}, \tag{15}$$

where $q = e^{2\pi i \tau}$, $\eta(\tau) = q^{1/24} \prod_{n=1}^{\infty} (1 - q^n)$ is the Dedekind function [26] and $\text{CZ}(\tau, \zeta) = \exp(-\pi \nu_H (\text{Im } \zeta)^2 / \text{Im } \tau)$ is the Cappelli–Zemba factor introduced to restore the invariance of $K_l(\tau, \zeta; m)$ with respect to the Laughlin spectral flow [29]. The $\widehat{u(1)}$ charge label l in $Z^{l,\Lambda}$ is determined by the total electric charge of the localized quasiparticles in the bulk $Q_{\text{el}}(\text{bulk}) = l/d_H$, while the weight Λ is determined by the total neutral topological charge of the quasiparticles localized in the bulk. The partition function $\text{ch}_{\Lambda}(\tau')$ represents the neutral edge modes corresponding to the total neutral topological charge Λ in the bulk. The modular parameter $\tau' = r\tau$ with $r = v_n/v_c$ is modified in order to take into account the observation [32,1] that the Fermi velocity v_n of the neutral edge modes might be smaller than v_c . The $*$ in $Z^{l,\Lambda}$ denotes the fusion product [26] of the topological charge Λ with the (s -multiple) neutral topological charge ω of the electron [25,30]. The electric charge of the edge excitations, with quantum numbers n and s , encoded in the partition function (14) is

$$Q_{\text{el}}(l, \Lambda, n, s) = \frac{l}{d_H} + s + n_H n, \tag{16}$$

where l is the number of fundamental quasiparticles in the bulk, s is the number of electrons on the edge and n is the number of clusters of n_H electron on the edge. The neutral topological weight Λ and the electric charge l have to satisfy a general \mathbb{Z}_{n_H} pairing rule, see Eq. (19) in [30],

$$n_H \tilde{Q}_{\omega}(\Lambda) \equiv l \pmod{n_H}, \tag{17}$$

where $\tilde{Q}_{\omega}(\Lambda)$ is the (neutral) monodromy charge defined by the following combination of conformal dimensions Δ_{Λ} of the neutral Virasoro irreducible representations

$$\tilde{Q}_{\omega}(\Lambda) \equiv \Delta_{\omega * \Lambda} - \Delta_{\Lambda} - \Delta_{\omega} \pmod{\mathbb{Z}}, \quad (\Delta_{\omega} = \Delta^{(0)}). \tag{18}$$

The \mathbb{Z}_{n_H} pairing rule (17), which selects the admissible pairs (l, Λ) of charged and neutral quantum numbers, follows from the locality condition for the short-distance operator product expansions of the physical excitations with respect to the neutral part $\psi_{\text{el}}^{(0)}(z)$ of the electron field [30] of CFT dimension $\Delta^{(0)}$, characterized by the neutral electron weight ω .

Next we can introduce the AB flux ϕ into the partition function (14) by the shift (8) and then move the flux and chemical potential dependences into the charge index of the K function (15), due to the identity [25]

$$K_l(\tau, \zeta + \phi\tau; m) \equiv K_{l+\phi}(\tau, \zeta; m), \tag{19}$$

setting $\zeta = 0$ after that, i.e. introducing AB flux ϕ leads to the index shift $l + sd_H \rightarrow l + sd_H + n_H \phi$, so that the partition function with AB flux ϕ is²

$$Z_{\phi}^{l,\Lambda}(\tau, \mu) \propto \sum_{s=0}^{n_H-1} \text{ch}_{\omega^s * \Lambda}(\tau') \sum_{n=-\infty}^{\infty} e^{-\beta \Delta \varepsilon \frac{n_H d_H}{2} \left(n + \frac{l + s d_H}{n_H d_H} + \frac{1}{d_H} \left(\phi + \frac{\mu}{\Delta \varepsilon} \right) \right)^2}. \tag{20}$$

² We skip the η -function and the CZ factor from Eq. (14) which are unimportant multiplicative factors for $\zeta = 0$.

In order to compute the average tunneling energy (6) we need to specify the parameters μ_N and μ_{N+1} corresponding to QD with N and $N + 1$ electrons, respectively. To this end we emphasize that the parameter μ entering (9) is not the true chemical potential, except at zero gate voltage, because it is not coupled to the electron number operator but to the charge imbalance N_{imb} [24].

As can be seen in Appendix B, when the bulk electron number is $N_0 = n_H n_0$, where n_0 is a positive integer and n_H is the numerator of the filling factor ν_H , the partition function (20) is independent of the bulk component of μ and the edge components of μ_N and μ_{N+1} can be chosen as

$$\mu_N = -\frac{\Delta\varepsilon}{2} \quad \text{and} \quad \mu_{N+1} = \frac{\Delta\varepsilon}{2}, \quad (21)$$

where $\Delta\varepsilon$ is the QD level spacing. This choice of μ_N and μ_{N+1} is universal in the sense that it is independent of the neutral contributions to the electron energy, or of the ratio $r = v_n/v_c$ of the Fermi velocities of the neutral and charged modes, or even of ν_H , see Appendix B for more detail.

4. Thermoelectric properties of a $\nu_H = 5/2$ CB island

We will illustrate the general approach to thermopower using as an example a $\nu_H = 5/2$ CB island, assuming that only the higher $\nu_H = 1/2$ edge is strongly backscattering, as in Ref. [1]. So far only the fractional electric charge $e/4$ of the fundamental quasiparticles has been confirmed experimentally [33–35] and this is consistent with several FQH candidates: the Pfaffian Moore–Read state [3], the anti-Pfaffian [36,37], the 331 Halperin state [38] and the $\widehat{u}(1) \times \widehat{SU}(2)_2$ state [39]. The difference between the Pfaffian and the $\widehat{SU}(2)_2$ state is only in the neutral sector: instead of the Ising model irreducible representations with CFT dimensions 0, 1/16 and 1/2 we use in the $\widehat{SU}(2)_2$ state the irreducible representation of the level-2 current algebra $\widehat{SU}(2)_2$ with CFT dimensions 0, 3/16 and 1/2, respectively. The electric properties of the Pfaffian and $\widehat{SU}(2)_2$ are the same, the fusion rules are the same, the CB peak patterns are the same in the zero temperature limit, yet they have significantly different thermoelectric properties which if measured in an experiment could help us to figure out which state is realized in nature. For our purposes, the most important things are the partition functions for the two models and they are explicitly written in Eqs. (25) and (27) below.

In the rest of this paper we will use the CFT partition functions to compute numerically the thermopower, conductance, thermal conductance and power factor for these FQH islands. The partition functions of the paired FQH states with $\nu_H = 5/2$ with quasiparticles in the bulk depend on their number modulo 2 (modulo n_H in general) [7,31,1]. Therefore we consider only two cases: even (no quasiparticles in the bulk) and odd (one quasiparticle in the bulk). We start with the case of one bulk quasiparticle (odd number), which is simpler than the case of zero bulk quasiparticles (even number).

4.1. Odd number of bulk quasiparticles

The partition functions for the paired³ $\nu_H = 1/2$ FQH states with odd number of quasiparticles in the bulk, e.g. with one quasiparticle in the bulk, is

³ We consider only the highest Landau level with $\nu_H = 1/2$ and $n_H = 2$, $d_H = 4$.

$$\begin{aligned} Z^{\text{odd}}(\tau, \zeta) &= K_1(\tau, 2\zeta; 8)\text{ch}_\sigma(\tau') + K_{-3}(\tau, 2\zeta; 8)\text{ch}_{\omega*\sigma}(\tau') \\ &= [K_1(\tau, 2\zeta; 8) + K_{-3}(\tau, 2\zeta; 8)]\text{ch}_\sigma(\tau'), \end{aligned} \quad (22)$$

where the K functions are defined in (15), $\text{ch}_\sigma(\tau')$ is the neutral partition function for the one-quasiparticle sector labeled by the topological charge σ of the basic quasihole in the FQH liquid, which could generate by fusion with itself all other quasiholes, and $\text{ch}_{\omega*\sigma}$ is the neutral partition function of the topological sector labeled by $\omega*\sigma$, with ω being the neutral topological charge of the electron field [25,30]. In all three cases of the Pfaffian, $SU(2)_2$ and Anti-Pfaffian the neutral characters satisfy $\text{ch}_{\omega*\sigma}(\tau') \equiv \text{ch}_\sigma(\tau')$ as a consequence of the fusion rules $\psi_{\text{el}}^{(0)} \times \sigma \simeq \sigma$, where σ is the lowest-CFT dimension quasiparticle field and $\psi_{\text{el}}^{(0)}$ is the electron field corresponding to the neutral topological weight ω . For the 331 state the sectors with σ and $\omega*\sigma$ are represented by different topological charges having opposite fermion parity, however the neutral partition functions of the two sectors coincide because $K_{-1}(\tau, 0; 4) \equiv K_1(\tau, 0; 4)$. Therefore in all four cases of paired FQH states, including the Anti-Pfaffian state, we have $\text{ch}_{\omega*\sigma}(\tau') \equiv \text{ch}_\sigma(\tau')$ which explains the second line of (22). Next we can use the identity⁴

$$K_{l+\frac{1}{2}}(\tau, \zeta; 2) \equiv K_{2l+1}(\tau, 2\zeta; 8) + K_{2l-3}(\tau, 2\zeta; 8) \quad (23)$$

to find that $K_1(\tau, 2\zeta; 8) + K_{-3}(\tau, 2\zeta; 8) = K_{1/2}(\tau, \zeta; 2)$ and the partition function (22) is written as a *single product* of a charged part $K_{1/2}(\tau, \zeta; 2)$ and a neutral part $\text{ch}_\sigma(\tau')$. It is now obvious that the neutral part of the CFT has no contribution to the average tunneling energy (4) for odd number of quasiparticles in the bulk and the distance between the centers of the consecutive peaks of the electric and thermal conductances is always $\Delta\phi = 2$, as shown in Fig. 3 below. This result is consistent with that of Ref. [1]. Therefore, the neutral degrees of freedom are completely decoupled from the charged ones and the thermoelectric properties are basically the same as for the $g = 1/2$ Luttinger liquid. This includes the anti-Pfaffian state, with odd number of bulk quasiparticles, as well, cf. [1]. Thus, the thermoelectric quantities of the paired states with odd number of bulk quasiparticles are not sensitive to the ratio $r = v_n/v_c$ of the Fermi velocities of the neutral and charged edge modes.

The thermopower for a Coulomb blockaded island, of paired $\nu_H = 5/2$ quantum Hall states with one quasiparticle in the bulk, as a function of the AB flux is computed numerically from Eqs. (2), (6), (11), (13) and (20) and is given graphically in Fig. 2. The thermopower oscillations are apparently similar to those of metallic islands except that the period in the normalized AB flux is $\Delta\phi = 2$ instead of 1. The peaks of the electrical conductance shown in Fig. 2 are equally spaced with period $\Delta\phi = 2$, the thermopower is zero at the centers of the conductance peaks and thermopower is disconnected (at $T = 0$) at the centers of the CB valleys, just like in metallic CB islands [12,41]. For comparison, the oscillation of the thermopower, for a CB island formed in a $\nu_H = 1/3$ Laughlin quantum Hall state with $l = 0$ and the CB conductance, can be seen in [14]. The thermopower in that case has a similar saw-tooth behavior with period 3 flux quanta and the positions of the CB peaks correspond to the zeros of the thermopower. cf. [12,41].

Due to Eq. (1) the thermal conductances peaks for all paired FQH states with odd number of bulk quasiparticles can be obtained from the calculated thermopower S and electrical conductance (12) by $G_T = G \cdot S$, see Fig. 3. They are also equally spaced, with period $\Delta\phi = 2$, are completely symmetric for all temperatures and are independent of $r = v_n/v_c$, showing similar results as in [1].

⁴ The relation (23) is not so obvious although it follows directly from Eq. (15). It is the odd-index version of a more general relation of Eq. (C.5) in Ref. [40].

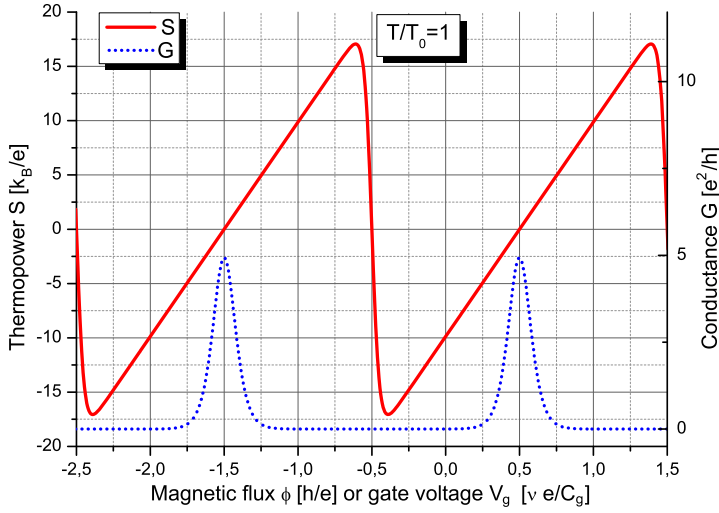


Fig. 2. Thermopower of a CB island for all paired states for $\nu_H = 5/2$, with odd number of quasiparticles in the bulk, including anti-Pfaffian, at temperature $T/T_0 = 1$.

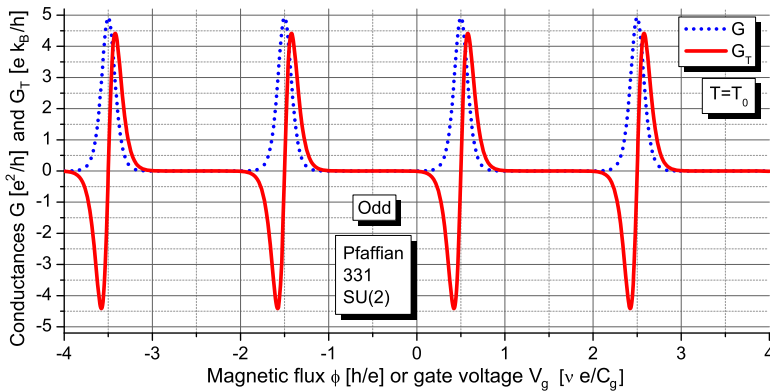


Fig. 3. Electric and thermal conductances G and $G_T = S.G$ for all paired FQH states with odd number of quasiparticles in the bulk, including the Anti-Pfaffian CB island at temperature $T/T_0 = 1$.

Finally, in Fig. 4 we plot the power factor \mathcal{P}_T for all paired states at $\nu_H = 5/2$ with odd number of bulk quasiparticles computed numerically at $T = T_0$ from Eq. (4), together with the peaks of the conductance (right-Y scale). The power factor shows sharp dips corresponding precisely to the maxima of the conductance peaks. Notice that this figure is qualitatively similar to Fig. 3c in Ref. [21], which suggests that the method used there for measuring the thermoelectric current might be convenient for measuring the power factors of for the $\nu_H = 5/2$ FQH state as well, see the discussion before Eq. (28).

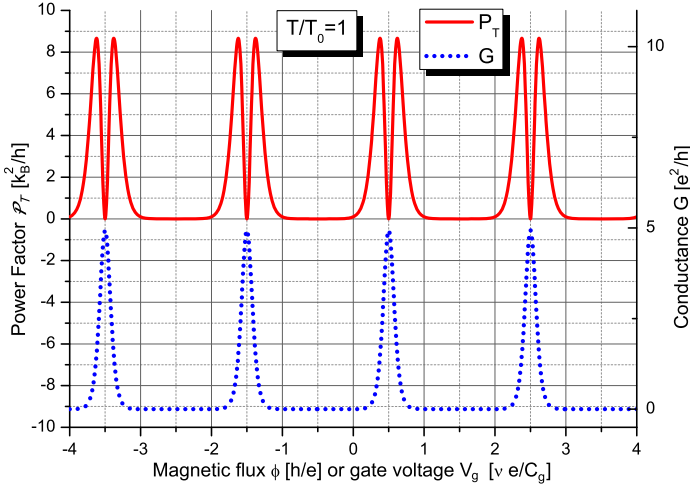


Fig. 4. The Power factor \mathcal{P}_T of a CB island for all paired states for $\nu_H = 5/2$, with odd number of quasiparticles in the bulk, including anti-Pfaffian, at temperature $T/T_0 = 1$.

4.2. Even number of bulk quasiparticles

The partition functions for a CB island in all paired FQH states with $\nu_H = 5/2$ with even number of quasiparticles in the bulk⁵ can be written as a sum of two products, e.g. for zero bulk quasiparticles,

$$Z^{\text{even}}(\tau, \zeta) = K_0(\tau, 2\zeta; 8)\text{ch}_0(\tau') + K_4(\tau, 2\zeta; 8)\text{ch}_\omega(\tau') \tag{24}$$

where $\tau' = r\tau$ with $r = v_n/v_c$, the K functions are defined in (15) and $\text{ch}_0(\tau')$ is the neutral partition function of the vacuum sector, while $\text{ch}_\omega(\tau')$ is the neutral partition function of the one-electron sector.

The neutral partition functions in (24) for the Pfaffian state can be expressed as

$$\begin{aligned} \text{ch}_0(\tau) &= \frac{q^{-1/48}}{2} \left(\prod_{n=1}^{\infty} (1 + q^{n-1/2}) + \prod_{n=1}^{\infty} (1 - q^{n-1/2}) \right), \\ \text{ch}_\omega(\tau) &= \frac{q^{-1/48}}{2} \left(\prod_{n=1}^{\infty} (1 + q^{n-1/2}) - \prod_{n=1}^{\infty} (1 - q^{n-1/2}) \right), \end{aligned} \tag{25}$$

where $q = e^{2\pi i\tau}$. Now that we have specified the complete partition function for the Pfaffian state without bulk quasiparticles we plot in Fig. 5 the electron number (11) and electric conductance (12) for the Pfaffian island without bulk quasiparticles as functions of the AB flux ϕ , respectively, of the gate voltage V_g . We see in Fig. 5 that the positions of the peaks of the electric conductance of the CB island precisely corresponds to the positions in gate voltage where the electron number on the island increases by one. For illustration purposes the two functions are computed for equal velocities of the neutral and charged edge modes, $v_n = v_c$, i.e. for $r = 1$ in which case the conductance peaks are packed in pairs of peaks separated by flux distance $\Delta\phi_1 = 1$ which

⁵ We consider only the highest Landau level with $\nu_H = 1/2$ and $n_H = 2$, $d_H = 4$.

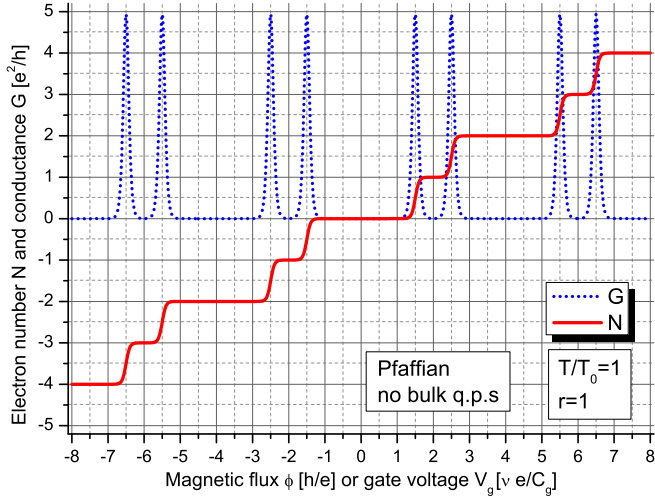


Fig. 5. Coulomb island conductance G and electron number N , measured from N_0 , of the Pfaffian FQH state at temperature $T = T_0$ for $\nu_n = \nu_c$. The number N jumps by 1 at the conductance peak positions.

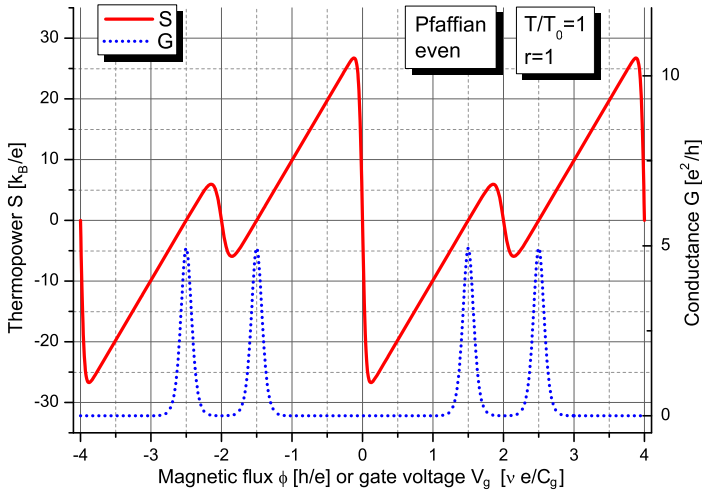


Fig. 6. Thermopower of a CB island in the Pfaffian state for $\nu_H = 5/2$, without quasiparticles in the bulk, for $r = 1$, at temperature $T/T_0 = 1$.

are then separated by a flux distance $\Delta\phi_2 = 2$ between the groups of peaks. When temperature is decreased the CB conductance peaks become higher and narrower while the profile of the electron number becomes closer to the step function.

The thermopower for a Coulomb blocked island in the Pfaffian state without bulk quasiparticles with $r = 1$ is computed from Eqs. (2), (6), (11), (13) and (20) and is given as a function of the gate voltage in Fig. 6, which is a central result in this work. Two important characteristics of the thermopower for fractional quantum Hall states have to be emphasized: when the gate voltage approaches a position of a CB peak the thermopower vanishes at the maximum of the peak, just like it does for metallic islands [12]; second, at the centers of the CB valleys thermopower

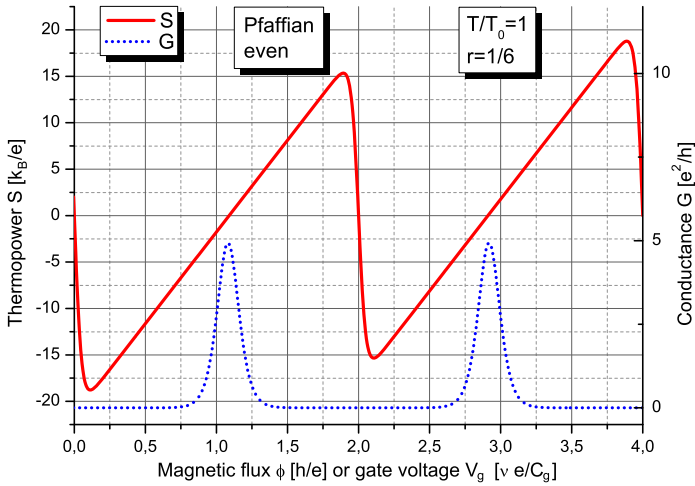


Fig. 7. Thermopower of a CB island in the Pfaffian state for $\nu_H = 5/2$, without quasiparticles in the bulk, for $r = 1/6$, at temperature $T/T_0 = 1$.

decreases rapidly (jumping discontinuously at $T = 0$) crossing the x -axis exactly at the center of the valley like in metallic islands [12]. This modified saw-tooth shape of the thermopower is similar to that in superconducting SET [42].

In addition to Fig. 6 showing the thermopower for the Pfaffian state with even number of bulk quasiparticles at $T = T_0$ and $r = 1$, we plot for comparison in Fig. 7 the thermopower for the same state (Pfaffian, even), however with $r = 1/6$. We see that the differences in the neighboring maxima of the thermopower, seen in Fig. 6, decreased for $r = 1/6$ and are probably hard to observe experimentally. However, still the zero's of the thermopower correspond to the maxima of the electric conductance. Again the CB peaks are not equally spaced and have two periods which are of the form $\Delta\phi_1 = 2 - r$ and $\Delta\phi_2 = 2 + r$, where $r = v_n/v_c$ is the ratio of the Fermi velocities of the neutral and charged edge modes. However, measuring the differences in CB peak spacing does not seem very promising from the experimental point of view.

The plot of the thermopower of the Anti-Pfaffian state is similar to that in Fig. 7 except that the positions of the higher and lower maxima of the thermopower are exchanged.

Next, we continue with the other paired FQH states. In order to completely define the corresponding total partition functions (24) for the edges of the CB island we need to specify the neutral partition functions. The neutral partition functions for a Coulomb blockaded island in the 331 state are expressed in terms of the K functions (15) as

$$\text{ch}_0(q) = K_0(\tau, 0; 4), \quad \text{ch}_\omega(q) = K_2(\tau, 0; 4), \tag{26}$$

while the neutral partition functions for the $SU(2)_2$ FQH state [39] are defined as the $\widehat{SU(2)}_2$ characters with lowest CFT dimensions 0 and 1/2 respectively, which are expressed in terms of the functions from Eq. (14.183) in Ref. [26]

$$\text{ch}_0(\tau) = \chi_0^{(2)}(\tau) = \frac{q^{\frac{1}{16}}}{\eta(q)^3} \sum_{n \in \mathbb{Z}} (1 + 8n) q^{n(1+4n)}$$

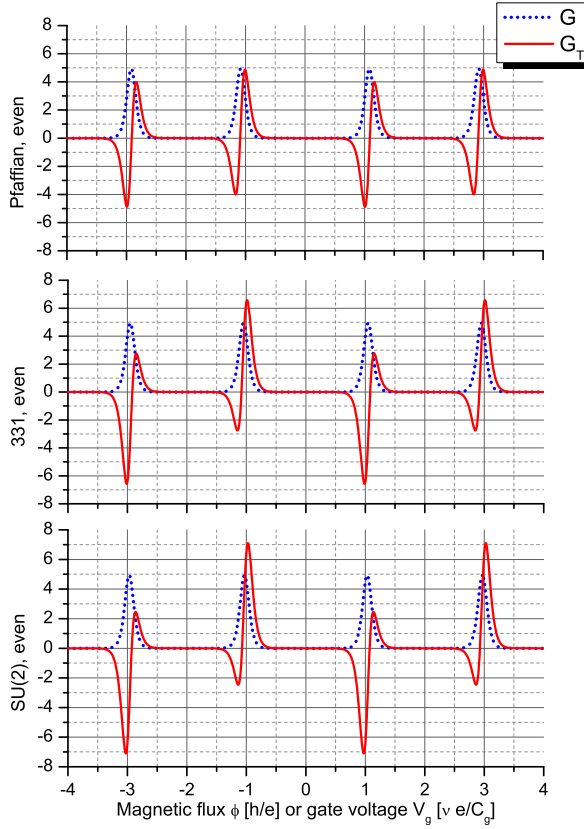


Fig. 8. Conductances G , in units $[e^2/h]$, and G_T , in units $[ek_B/h]$, for the Pfaffian, 331 and $SU(2)_2$ models without quasiparticles in the bulk, with $r = 1/6$, at temperature $T/T_0 = 1$.

$$\text{ch}_\omega(\tau) = \chi_2^{(2)}(\tau) = \frac{q^{\frac{9}{16}}}{\eta(q)^3} \sum_{n \in \mathbb{Z}} (3 + 8n) q^{n(3+4n)}. \tag{27}$$

In Fig. 8 we plotted the electric and thermal conductances for the Pfaffian, 331 and $SU(2)_2$ states with even number of quasiparticles in the bulk at $T = T_0$ for $r = v_n/v_c = 1/6$. We see that the zeros of the thermal conductances G_T coincide with the maxima of the corresponding electric conductances' peaks and then G_T changes sign. However, unlike the case with odd number of bulk quasiparticles, where the peaks were equally spaced, here there are again the two periods $\Delta\phi_1 = 2 - r$ and $\Delta\phi_2 = 2 + r$, depending on the ratio $r = v_n/v_c$ of the Fermi velocities of the neutral and charged edge modes. The oscillations of the thermal conductances in Fig. 8 are apparently asymmetric which is a consequence of the asymmetries in the thermopower. These asymmetries are signals that the neutral degrees of freedom play an important role for the paired FQH states with even number of bulk quasiparticles [10,1].

As pointed out in Ref. [1] the ratio of the amplitudes of the minimum and maximum of the thermal conductance G_T could serve as an experimental signature that could eventually distinguish between the different paired FQH states having the same electric conductance peak patterns. Below we will demonstrate that the ratio of the neighboring maxima of the power factor (4) around a CB peak position, computed from the thermopower and the conductances, might be

a better tool to distinguish between these FQH states. We argue that this quantity could be measured by the method of Ref. [21] where the N-gate input AC voltage V_N has frequency $f_0/2 = 497.5$ kHz, while the transmission coefficient is measured for the output current at frequency $f_0 = 995$ kHz. We claim that the measured signal shown in Fig. 3c in Ref. [21] is actually proportional to the power factor (4). Indeed, the measured current is of the form $I = G\Delta V + G_T\Delta T$, where ΔV is the QD bias which we assume to be very small and the voltage induced temperature difference is $\Delta T = \alpha|V_N|$ for small ΔT , as can be seen in Fig. 2c in Ref. [21]. The voltage on gate N in the setup of Ref. [21] is of the form $V_N = V_{N,DC} + V_{N,AC} \cos(2\pi(f_0/2)t)$ and in the regime where the input frequency is half of that of the measured output signal $V_{N,DC}$ is set to 0. When the input signal V_N is at frequency $f_0/2$ and the output is measured at f_0 we are actually measuring the square of the current, which is $I^2 \propto V_{N,AC}^2/2 \cos(2\pi f_0 t)$. On the other hand, if we consider the power of the thermoelectric current⁶

$$P = GI^2 \propto \alpha^2 G \cdot S^2 V_N^2 \propto P_T \cos(2\pi f_0 t), \quad (28)$$

we see that the term in front of $\cos(2\pi f_0 t)$ is proportional to the power factor P_T defined in (4). Thus we conclude that the signal shown in Fig. 3c in Ref. [21] is proportional to the power factor (4) for $\nu_H = 2/3$ which is similar to our Fig. 4. Therefore we are confident that this procedure gives a nice method for direct measuring the power factor of a QD. Next, we show in Fig. 9 the power factors for the Pfaffian, 331 and $SU(2)_2$ models without quasiparticles in the bulk, with $r = 1/6$, at temperature $T/T_0 = 1$. We emphasize here that, due to the asymmetries mentioned earlier, the plots of the power factors for the different paired states candidates describing the $\nu_H = 5/2$ FQH state are noticeably different for the different FQH states even for $r = 1/6$ when the electric conductance patterns are indistinguishable. Therefore we strongly believe that the power factor (4) is a better spectroscopic tool than the electric and thermal conductances alone, which might eventually be used to experimentally distinguish between the different candidate states for $\nu_H = 5/2$.

For comparison with Fig. 9 and Fig. 4 we also plot in Fig. 10 the power factor \mathcal{P}_T computed from Eq. (4) for the Pfaffian state without bulk quasiparticles again at $T = T_0$, however this time for $r = 1$. We see that again the sharp dips in the power factor correspond to the maxima of the conductance peaks but for $\nu_n = \nu_c$ the ratio of the two maxima of \mathcal{P}_T around a conductance peak is obviously 1. As mentioned before, the sharp zeros of the power factor can be used to determine experimentally the ratio $r = \nu_n/\nu_c$ because the CB peak pattern for all paired FQH states proposed for $\nu_H = 5/2$ with even number of bulk quasiparticles [31,1] consists of a longer flux period $\Delta\phi_2 = 2 + r$ and a shorter one $\Delta\phi_1 = 2 - r$, as shown in Fig. 10, while that for the states with odd number of bulk quasiparticles is equidistant, i.e., $\Delta\phi_1 = \Delta\phi_2 = 2$. This equidistant pattern of CB peaks could be used as a reference [31,11,10,1]. Since, according to Eq. (8), the gate voltage V_g is simply proportional to the AB flux ϕ we have that the ratio of the gate voltage periods is the same, i.e., $x = \Delta V_2/\Delta V_1 = \Delta\phi_2/\Delta\phi_1 \geq 1$ and therefore

$$r = \lim_{T \rightarrow 0} 2 \frac{(\Delta V_2/\Delta V_1) - 1}{(\Delta V_2/\Delta V_1) + 1}. \quad (29)$$

For experimental purposes the ratio $2(x-1)/(x+1)$ at temperatures $T \leq T_0/2$ is very close to its zero-temperature value.

We also plot in Fig. 11 the power factor for the Anti-Pfaffian state with $r = 1/6$ at $T = T_0$ computed from the partition function of Ref. [9,1]. We considered the partition function for the

⁶ We assume that the bias is $\Delta V \simeq 0$.

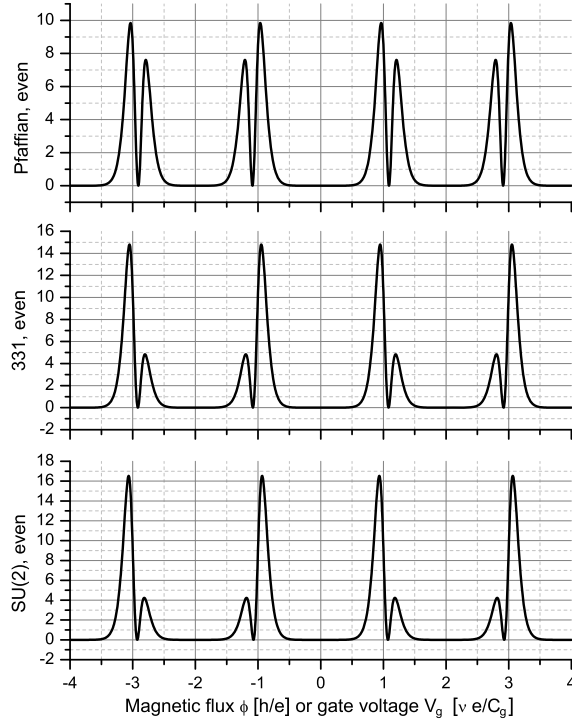


Fig. 9. Power factors \mathcal{P}_T , in units $[k_B^2/h]$, for the Pfaffian, 331 and $SU(2)_2$ models without quasiparticles in the bulk, with $r = 1/6$, at temperature $T/T_0 = 1$.

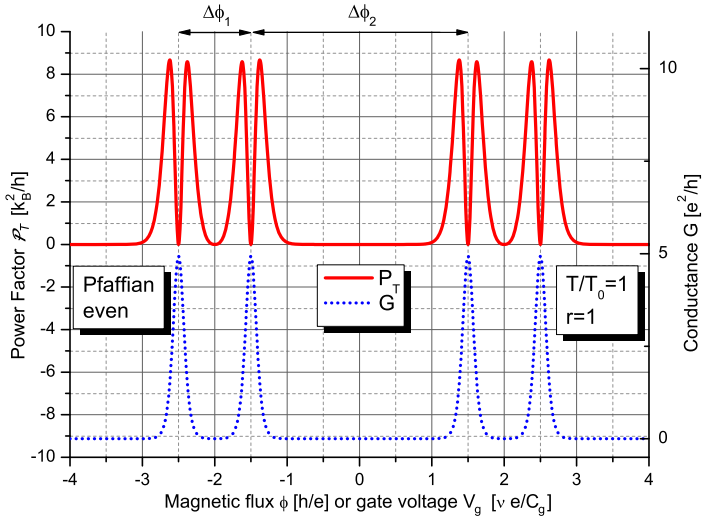


Fig. 10. The Power factor \mathcal{P}_T of a CB island for the Pfaffian state for $\nu_H = 5/2$, without quasiparticles in the bulk, with $r = 1$, at temperature $T/T_0 = 1$.

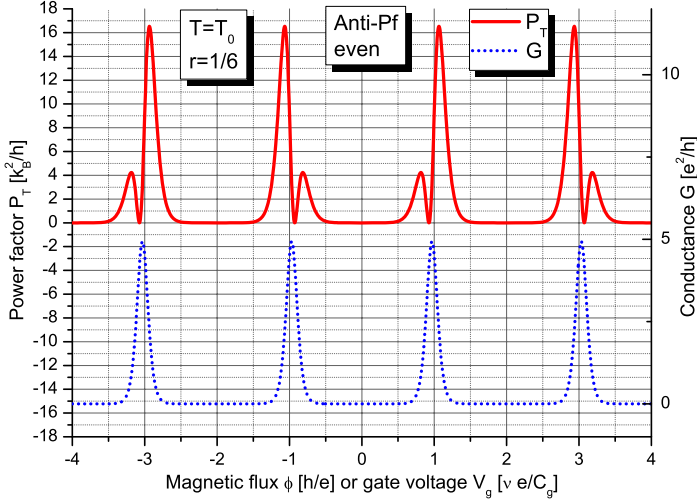


Fig. 11. The Power factor \mathcal{P}_T and the conductance G of a CB island for the Anti-Pfaffian state for $\nu_H = 5/2$, without quasiparticles in the bulk, with $r = 1/6$, at temperature $T/T_0 = 1$.

disorder-dominated phase of the Anti-Pfaffian state [37,36] with even number of bulk quasiparticles, in which the charged and neutral modes have already equilibrated [43,44] and consequently the Hall conductance is universal, as that of Eq. (24) with $ch_0 = [\chi_0^{(2)}]^{-1}$ and $ch_\omega = [\chi_2^{(2)}]^{-1}$, where $\chi_l^{(2)}$ are given in Eq. (27). Again the sharp dips of \mathcal{P}_T mark precisely the maxima of the conductance peaks and can be used to determine precisely their positions. The plot in Fig. 11 has to be compared with the power factors of the other paired states given in Fig. 4 and Fig. 9. The power factor for the Anti-Pfaffian state with even number of bulk quasiparticles is similar to that of the $SU(2)_2$ state though the places of higher and lower peaks, respectively the short and long periods in the gate voltage, are exchanged. This leads to different behavior of the ratio P_1^{\max}/P_2^{\max} , as shown in Fig. 12 which is also a clear signature of the Anti-Pfaffian or $SU(2)_2$ state.

Furthermore, the apparent asymmetries in \mathcal{P}_T might allow to distinguish between the different states by measuring the ratio P_1^{\max}/P_2^{\max} between the maxima of \mathcal{P}_T surrounding the first CB conductance peak with $\phi > 0$. The plot of these ratios as functions of T , for the Pfaffian, 331, $SU(2)_2$ and the anti-Pfaffian states, are shown in Fig. 12. Measuring P_1^{\max}/P_2^{\max} , as in [21], at three different temperatures, would be sufficient to determine experimentally one paired state among the others which is the best candidate to describe the universality class of the $\nu_H = 5/2$ FQH state. Of course, the ratios of the maxima of the power factor around a conductance peak can be recalculated if the ratio $r = \nu_n/\nu_c$, measured through Eq. (29), is different from $1/6$.

5. Discussion

We demonstrated that the CFT partition functions of Coulomb blocked FQH islands can be efficiently used to calculate the thermoelectric characteristics of the islands which could eventually distinguish between inequivalent FQH universality classes with similar CB peaks patterns, at finite temperature even when $\nu_n/\nu_c < 1$.

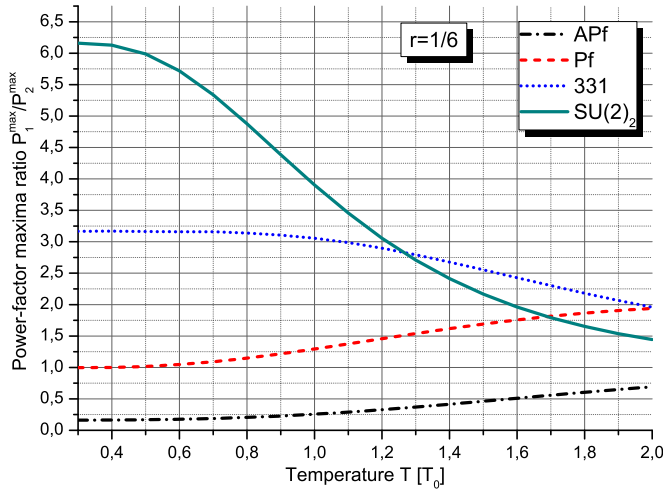


Fig. 12. Power-factor maxima ratio P_1^{\max}/P_2^{\max} of a CB island for all paired states for $\nu_H = 5/2$, without quasiparticles in the bulk, with $r = 1/6$, as functions of temperature T/T_0 .

In this work we have considered only chiral FQH states. The only exception is the Anti-Pfaffian state for which we have used the partition function given in Refs. [9,1]. The reason is that for the chiral FQH states all edge modes move in the same direction, which is determined by the direction of the magnetic field perpendicular to the FQH sample, and there is certainly a unitary rational CFT describing the edge states [15–18,9]. For the non-chiral FQH states, such as the $\nu_H = 2/3$ [43,21] and probably $\nu_H = 5/2$ as well [37,36,45], there might be counter-propagating neutral modes, or upstream modes, and it is not completely clear if conformal symmetry exists in the limit $v_n/v_c \rightarrow 1$, so that the effective field theory partition function is unknown. If the $\nu_H = 2/3$ FQH state is indeed the PH conjugate of the $\nu_H = 1/3$ Laughlin state then it certainly has counter-propagating modes. However, for most filling factors there are usually more than one candidate, and even if the experiments and numerical calculations favor one candidate there are phase transitions, etc; For example, in a recently proposed new Abelian candidate for $\nu_H = 5/2$, referred to as the 113 Halperin state [46], the standard partition function is divergent because the K -matrix is not positive definite. There are also some open problems, such as equilibration of counter-propagating modes in disorder-dominated phases, non-universality of the Hall conductance without equilibration, edge reconstruction, etc. However, as soon as the partition function for any FQH state is fixed the method described here would allow to compute the thermopower, figure-of-merit, power factor and conductances of a Coulomb-blockaded island inside this state.

It is worth mentioning that we consider the case $v_n = v_c$ as a “zero approximation” and admit that interactions could renormalize both velocities, so the conformal symmetry exists exactly in this initial approximation. The important point here is that we expect that the structure of the Hilbert space of the edge states remain the same even after the renormalization so that we can use the same characters as partition function and simply change the modular parameter τ in order to take into account the different velocities. There is a proof in Ref. [18] that when all modes propagate in the same direction there is certainly conformal symmetry on the edge. The case with counter-propagating modes is not considered there and is unclear. If there is no CFT we do not know how to write the neutral partition functions, but if we knew them we could apply the approach described in this paper to compute the thermoelectric properties of the QD.

We conclude that the asymmetries in the power factor of Coulomb blockaded islands seem to be rather sensitive to the neutral degrees of freedom of the underlying edge states' effective conformal field theory and this could be used to determine experimentally which one of the candidate paired states describes best the fractional quantum Hall state at filling factor $\nu_H = 5/2$.

Acknowledgements

I thank Andrea Cappelli, Guillermo Zemba and Ady Stern for helpful discussions. This work has been partially supported by the Alexander von Humboldt Foundation under the Return Fellowship and Equipment Subsidies Programs and by the Bulgarian Science Fund under Contract No. DFNI-T02/6.

Appendix A. Additional details on Aharonov–Bohm twisting

Introducing AB flux $\phi = e(BA - B_0A_0)/h$ through the AB relation modifies the electron field by $\psi_{\text{el}}(z) \rightarrow z^{-\phi} \psi_{\text{el}}(z)$, where $z = e^{i\varphi}$ is the electron coordinate on the edge circle, see Section 2.8 in [25]. This *twisting* of the electron operator can be implemented by a conjugation [25] with a flux-changing operator U_β (here $\beta \in \mathbb{R}$ is the twist parameter and should not be confused with the inverse temperature) defined by its commutation relations with the Laurent modes of the normalized⁷ charge density $J(z) = \sum_{n \in \mathbb{Z}} J_n z^{-n-1}$, namely $[J_n, U_\beta] = \beta U_\beta \delta_{n,0}$. It is not difficult to see that U_β acts on the electron as $\psi_{\text{el}}(z) \rightarrow U_\beta \psi_{\text{el}}(z) U_{-\beta} = z^{-\phi} \psi_{\text{el}}(z)$ when the twist is $\beta = -\sqrt{\nu_H} \phi$ [25]. Then, the twisted electric charge is obtained by the same action [25] $J_0^{\text{el}} \rightarrow U_\beta J_0^{\text{el}} U_{-\beta} = J_0^{\text{el}} + \nu_H \phi$ and the twisted Hamiltonian, which is defined as [25] $H_{\text{CFT}} \rightarrow U_\beta H_{\text{CFT}} U_{-\beta} = H_{\text{CFT}} + \Delta \varepsilon \phi J_0^{\text{el}} + \Delta \varepsilon \nu_H \phi^2 / 2$, reproduces Eq. (10) while the twisted partition function is expressed as in Eq. (9).

In order to make connection with the notation of Ref. [25], whose results for the AB transformation will be used below, we denote $q = e^{2\pi i \tau} = e^{-\beta \Delta \varepsilon}$ and $e^{2\pi i \zeta} = e^{\beta \mu}$.

The form of the twisted Hamiltonian $H_{\text{CFT}}(\phi)$ defined in Eq. (10) is typical (see, e.g. Eq. (17) in Ref. [47]) for two-dimensional interacting electron systems in which single-particle energies depend quadratically on the orbital momentum n and hence depend quadratically on the AB flux after the shift [47] $n \rightarrow n - \phi$. Also we emphasize that while N_{el} denotes the electron number operator, in case when the AB flux is non-zero, the operator N_{imb} , defined in (10), is equal to the charge imbalance operator [24], i.e. it is the difference between the true electron number operator, which changes only by integers, and the externally induced charge $\nu_H \phi$, which varies continuously (either by external gate voltage or AB flux variation). To understand their relation physically we note that for $\phi = 0$ the derivative of the Grand potential $\Omega = -k_B T \ln Z$ w.r.t. μ is

$$\begin{aligned} \frac{\partial \Omega}{\partial \mu} &= \frac{1}{Z} \sum_{s=0}^{n_H-1} \frac{\text{ch}_{\omega^s * \Lambda}}{\eta(\tau)} \sum_{n \in \mathbb{Z}} \left(n_H n + s + \frac{l}{d_H} \right) \\ &\quad \times e^{-\beta \Delta \varepsilon \frac{n_H d_H}{2} \left(n + \frac{l + s d_H}{n_H d_H} \right)^2} e^{2\pi i n_H \zeta \left(n + \frac{l + s d_H}{n_H d_H} \right)}, \end{aligned} \quad (\text{A.1})$$

and by definition should be equal to $-\langle N_{\text{imb}} \rangle_{\beta, \mu}$. When we introduce AB flux by the shift (8) the K functions in $Z^{l, \Lambda}$ transform as

⁷ This means that the Laurent modes J_n of the normalized charge density $J(z) = \sum_{n \in \mathbb{Z}} J_n z^{-n-1}$ satisfy $[J_n, J_m] = n \delta_{n+m,0}$.

$$K_{l+sd_H}(\tau, n_H \zeta; n_H d_H) \rightarrow K_{l+sd_H}(\tau, n_H(\zeta + \phi\tau); n_H d_H).$$

However, the latter is equal to $K_{l+sd_H+n_H\phi}(\tau, n_H \zeta; n_H d_H)$ due to the K -function identity (19) i.e., the effect of adding AB flux is simply to shift the K -function index $l \rightarrow l + n_H \phi$. Then shifting l in (A.1) yields in the sum an extra term proportional to ϕ which after the average gives rise to

$$\frac{\partial \Omega_\phi}{\partial \mu} = -\langle N_{\text{el}}(\phi) \rangle_{\beta, \mu} + v_H \phi = -\langle N_{\text{imb}}(\phi) \rangle_{\beta, \mu}, \quad (\text{A.2})$$

that explains Eqs. (11) and (10). It is interesting to note that the operator $Q_{\text{imb}} \equiv -N_{\text{imb}}$ coincides with the zero mode of the twisted $u(1)$ current $\pi_\phi(J_0^{\text{el}})$ defined in [25], which is precisely the operator that appears in the twisted partition function (9) as coupled to μ . The electron number N_{el} on the edge of a Pfaffian CB island without quasiparticles in the bulk, computed numerically from Eq. (11) in the text, is shown in Fig. 5 together with the electric conductance G of the island computed from Eq. (12) for $l = 0$ and $\Lambda = 0$, at $\mu = 0$ and $r = 1$, as functions of the magnetic flux.

Appendix B. Fixing chemical potentials μ_N and μ_{N+1}

Now we continue with the explanation why we choose $\mu_N = -\Delta\varepsilon/2$ and $\mu_{N+1} = \Delta\varepsilon/2$. First, let us see why the partition function (20) is independent of the bulk chemical potential μ_0 but depends only on the edge part $\mu = \mu_{\text{tot}} - \mu_0$ as stated in the text. The electron number average derived in general from (A.2) with a total chemical potential $\mu_{\text{tot}} = \mu_0 + \mu$

$$\langle N(\phi) \rangle_{\beta, \mu} = -\frac{\partial \Omega_\phi}{\partial \mu} + v_H \left(\frac{\mu_{\text{tot}}}{\Delta\varepsilon} + \phi \right) = N_0 + \langle N_{\text{el}}(\phi) \rangle_{\beta, \mu},$$

contains a bulk term $v_H \mu_0 / \Delta\varepsilon$ and an edge term $v_H \mu / \Delta\varepsilon - \partial \Omega_\phi / \partial \mu$. Because the bulk term, corresponding to $\phi = 0$, must be equal to N_0 we find $\mu_0 = d_H \Delta\varepsilon N_0 / n_H$. Next we assume, as in the text, that the number of electrons in the bulk is $N_0 = n_H n_0$, where n_0 is a positive integer, so that the bulk chemical potential becomes $\mu_0 / \Delta\varepsilon = n_0 d_H$. Now, if we substitute μ_{tot} into the partition function (20) we see that the latter is independent of the bulk chemical potential μ_0 because the sum over n is invariant with respect to the shift $n \rightarrow n + n_0$, i.e., $Z_\phi^{l, \Lambda}(\tau, \mu_0 + \mu) = Z_\phi^{l, \Lambda}(\tau, \mu)$. Therefore the edge partition function (20), as well as all thermodynamic averages, depend only on the edge part μ of the total chemical potential $\mu_{\text{tot}} = \mu_0 + \mu$.

In order to determine the values of μ_N and μ_{N+1} , which are needed for the computation of the thermodynamic averages of the energy $H_{\text{CFT}}(\phi)$ and the electron number $N_{\text{el}}(\phi)$, we argue that the difference $\mu_{N+1} - \mu_N$ corresponds to the difference between the energy of the last occupied single-particle state in the CB island and the first available unoccupied single-particle state. This difference is proportional to the flux difference between the two states, i.e. $\mu_{N+1} - \mu_N = \phi \Delta\varepsilon$. The first unoccupied single-particle state in the QD can be obtained from the last occupied one by the Laughlin spectral flow [29]: we apply the Laughlin argument [48] to the last occupied single particle state by changing adiabatically the AB flux threading the electron disk from 0 to 1; when the flux becomes 1 the discrete spectrum of the Hamiltonian $H_{\text{CFT}}(\phi)$ becomes the same as the spectrum for $\phi = 0$ while the single-electron states are mapped onto themselves, i.e., if at $\phi = 0$ an electron is described by the (unnormalized) wave function $z^l e^{-|z|^2/4}$, then at $\phi = 1$ it would have the wave function $z^{l+1} e^{-|z|^2/4}$. Therefore the difference between the two chemical potentials corresponding to the last occupied and the first unoccupied single-particle states is

exactly $\mu_{N+1} - \mu_N = \Delta\varepsilon$. Put another way, the Laughlin spectral flow, which transforms the last occupied single-particle level to the first unoccupied one, is expressed by the (modular) transformation [29] $\zeta \rightarrow \zeta + \tau$ and it can be implemented by Eq. (8) with $\phi = 1$. Taking into account that $\zeta = (\mu/\Delta\varepsilon)\tau$, as defined in the text before Eq. (8), we conclude that the Laughlin spectral flow is equivalent to $(\mu/\Delta\varepsilon) \rightarrow (\mu/\Delta\varepsilon) + 1$, or $\mu \rightarrow \mu + \Delta\varepsilon$ so that $\Delta\mu = \Delta\varepsilon$. Next, assuming that $\mu_N + \mu_{N+1} = 0$, which is equivalent to fixing the QD in the center of a CB valley for $\phi = 0$, we finally obtain $\mu_N = -\Delta\varepsilon/2$ and $\mu_{N+1} = \Delta\varepsilon/2$ as in Eq. (21). It is worth stressing that $\mu_{N+1} - \mu_N$ is independent of the neutral degrees of freedom of the electrons in the QD, hence it is independent of the ratio $r = v_n/v_c$ of the Fermi velocities of the charged and neutral edge modes. It is also independent of the filling factor ν_H . Note however that, except for $\phi = 0$, μ_N is not the true chemical potential, because it is coupled in the partition function (9) to the charge imbalance operator N_{imb} defined in (10) instead of the particle number N_{el} . That is why, $\mu_{N+1} - \mu_N$ is not equal to the addition energy $\Delta\mu^{\text{phys}} = \mu_{N+1}^{\text{phys}} - \mu_N^{\text{phys}}$, where μ_N^{phys} is the true (physical) chemical potential. On the other hand, the addition energy $\Delta\mu_N^{\text{phys}}$ corresponds to the energy spacing between CB peaks and it can be interpreted as the difference between the energies of the ground states with $N + 1$ and N electrons and certainly depends on the neutral degrees of freedom and on the filling factor ν_H .

Appendix C. Electric charge and Luttinger liquid number for general FQH states

The modular parameter ζ in Eq. (20) carries an additional multiplicative factor n_H , the numerator of the filling factor $\nu_H = n_H/d_H$, which can be understood as follows [30]: the K functions (15) entering the full partition functions (20) are actually the partition functions for the Luttinger liquid which can be described by a chiral boson with a compactification radius [29] $R_c = 1/m$, where $m = n_H d_H$. This is because the $\widehat{u}(1)$ component of the electron field $e^{i\phi(z)/\sqrt{\nu_H}}$, which is fixed by the requirement to have electric charge 1, has a statistical angle $\theta/2\pi = d_H/n_H$ that is not integer for $n_H > 1$. Therefore, for $n_H > 1$ we need to consider a smaller chiral subalgebra containing only clusters of n_H electrons [30], which can be generated by $e^{in_H\phi(z)/\sqrt{\nu_H}} \simeq e^{i\sqrt{n_H d_H}\phi(z)}$. These fields have integer statistics and are local, however their corresponding $\widehat{u}(1)$ compactification radius $n_H d_H$ is bigger [30]. The electric charge operator Q can be expressed in terms of the normalized chiral $\widehat{u}(1)$ charge J_0 by $Q = \sqrt{\nu_H} J_0$. On the other hand the normalized charge J_0 is related to the Luttinger liquid number operator $N = -J_0/\sqrt{m}$, whose spectrum appears in the Luttinger liquid partition function (15) as a conjugate of ζ , so that combining both we can express Q by N as follows

$$Q = \sqrt{\frac{n_H}{d_H}} J_0 = -\sqrt{\frac{n_H}{d_H}} \sqrt{n_H d_H} N = -n_H N.$$

This implies that the modular parameter ζ in the partition function (20) must be multiplied by n_H . This detail has one important consequence: the charge index $l + sd_H$, which is divided by $n_H d_H$ in (20), is deformed by adding $n_H\phi$ in presence of extra AB flux. Therefore the AB flux enters (A.2) as $\phi n_H/d_H$ which is necessary for the correct implementation of the charge-flux relation in general FQH states [49,50,30].

References

- [1] G. Viola, S. Das, E. Grosfeld, A. Stern, Thermoelectric probe for neutral edge modes in the fractional quantum Hall regime, *Phys. Rev. Lett.* 109 (2012) 146801.

- [2] B. Blok, X.-G. Wen, Many-body systems with non-Abelian statistics, *Nucl. Phys. B* 374 (1992) 615.
- [3] G. Moore, N. Read, Nonabelions in the fractional quantum Hall effect, *Nucl. Phys. B* 360 (1991) 362.
- [4] N. Read, E. Rezayi, Beyond paired quantum Hall states: parafermions and incompressible states in the first excited Landau level, *Phys. Rev. B* 59 (1998) 8084.
- [5] S.D. Sarma, M. Freedman, C.N. Stiven, H. Simon, A. Stern, Non-Abelian anyons and topological quantum computation, *Rev. Mod. Phys.* 80 (2008) 1083, arXiv:0707.1889.
- [6] A. Stern, Anyons and the quantum Hall effect – a pedagogical review, *Ann. Phys.* 323 (2008) 204–249, arXiv:0711.4697.
- [7] R. Ilan, E. Grosfeld, A. Stern, Coulomb blockade as a probe for non-Abelian statistics in Read–Rezayi states, *Phys. Rev. Lett.* 100 (2008) 086803.
- [8] R. Ilan, E. Grosfeld, K. Schoutens, A. Stern, Experimental signatures of non-Abelian statistics in clustered quantum Hall states, *Phys. Rev. B* 79 (2009) 245305, arXiv:0803.1542.
- [9] A. Cappelli, G. Viola, Partition functions of non-Abelian quantum Hall states, *J. Phys. A, Math. Theor.* 44 (7) (2011) 075401.
- [10] L.S. Georgiev, Thermal broadening of the Coulomb blockade peaks in quantum Hall interferometers, *Europhys. Lett.* 91 (2010) 41001, arXiv:1003.4871.
- [11] P. Bonderson, C. Nayak, K. Shtengel, Coulomb blockade doppelgangers in quantum Hall states, *Phys. Rev. B* 81 (2010) 165308, arXiv:0909.1056.
- [12] K. Matveev, Thermopower in quantum dots, *Lect. Notes Phys.* 547 (1999) 3–15.
- [13] C.W.J. Beenakker, A.A.M. Staring, Theory of the thermopower of a quantum dot, *Phys. Rev. B* 46 (1992) 9667–9676, <http://dx.doi.org/10.1103/PhysRevB.46.9667>.
- [14] L.S. Georgiev, Thermopower in the Coulomb blockade regime for Laughlin quantum dots, arXiv:1406.5592, 2014.
- [15] X.-G. Wen, Topological order in rigid states, *Int. J. Mod. Phys. B* 4 (1990) 239.
- [16] J. Fröhlich, T. Kerler, Universality in quantum Hall systems, *Nucl. Phys. B* 354 (1991) 369.
- [17] A. Cappelli, C.A. Trugenberger, G.R. Zemba, Infinite symmetry in the quantum Hall effect, *Nucl. Phys. B* 396 (1993) 465.
- [18] N. Read, Conformal invariance of chiral edge theories, *Phys. Rev. B* (2009) 245304.
- [19] A. Staring, L. Molenkamp, B. Alphenhaer, H. van Houten, O. Buyk, M. Mabesoone, C. Beenakker, C. Foxon, Coulomb-blockade oscillations in the thermopower of a quantum dot, *Europhys. Lett.* 22 (1993) 57.
- [20] Y. Dubi, M. Di Ventra, Colloquium: heat flow and thermoelectricity in atomic and molecular junctions, *Rev. Mod. Phys.* 83 (2011) 131–155, <http://dx.doi.org/10.1103/RevModPhys.83.131>.
- [21] I. Gurman, R. Sabo, M. Heiblum, V. Umansky, D. Mahalu, Extracting net current from an upstream neutral mode in the fractional quantum Hall regime, *Nat. Commun.* 3 (2012) 1289, arXiv:1205.2945.
- [22] J. Liu, Q.-f. Sun, X.C. Xie, Enhancement of the thermoelectric figure of merit in a quantum dot due to the Coulomb blockade effect, *Phys. Rev. B* 81 (2010) 245323, <http://dx.doi.org/10.1103/PhysRevB.81.245323>.
- [23] L.P. Kouwenhoven, D.G. Austing, S. Tarucha, Few-electron quantum dots, *Rep. Prog. Phys.* 64 (2001) 701–736.
- [24] H. van Houten, C. Beenakker, A. Staring, Single Charge Tunneling, NATO ASI Series, vol. B294, Plenum, New York, 1992, arXiv:cond-mat/0508454.
- [25] L.S. Georgiev, A universal conformal field theory approach to the chiral persistent currents in the mesoscopic fractional quantum Hall states, *Nucl. Phys. B* 707 (2005) 347–380, arXiv:hep-th/0408052.
- [26] P. Di Francesco, P. Mathieu, D. Sénéchal, Conformal Field Theory, Springer-Verlag, New York, 1997.
- [27] V. Kac, I. Todorov, Affine orbifolds and rational conformal field theory extensions of $W_{1+\infty}$, *Commun. Math. Phys.* 190 (1997) 57–111.
- [28] R. Kubo, M. Toda, N. Hashitsume, Statistical Physics II, Springer-Verlag, Berlin, 1985.
- [29] A. Cappelli, G.R. Zemba, Modular invariant partition functions in the quantum Hall effect, *Nucl. Phys. B* 490 (1997) 595, arXiv:hep-th/9605127.
- [30] L.S. Georgiev, Hilbert space decomposition for Coulomb blockade in Fabry–Pérot interferometers, arXiv:1112.5946, 2011.
- [31] A. Cappelli, G. Viola, G.R. Zemba, Chiral partition functions of quantum Hall droplets, *Ann. Phys.* 325 (2010) 465, arXiv:0909.3588.
- [32] X. Wan, Z.-X. Hu, E.H. Rezayi, K. Yang, Fractional quantum Hall effect at $\nu = 5/2$: ground states, non-Abelian quasiholes, and edge modes in a microscopic model, *Phys. Rev. B* 77 (2008) 165316, <http://dx.doi.org/10.1103/PhysRevB.77.165316>.
- [33] M. Dolev, M. Heiblum, V. Umansky, A. Stern, D. Mahalu, Observation of a quarter of an electron charge at the $\nu = 5/2$ quantum Hall state, *Nature* 452 (2008) 829.
- [34] I.P. Radu, J.B. Miller, C.M. Marcus, M.A. Kastner, L.A. Pfeiffer, K.W. West, Quasi-particle properties from tunneling in the $\nu = 5/2$ fractional quantum Hall state, *Science* 320 (2008) 899.

- [35] R.L. Willett, L.N. Pfeiffer, K.W. West, Alternation and interchange of $e/4$ and $e/2$ period interference oscillations consistent with filling factor $5/2$ non-Abelian quasiparticles, Phys. Rev. B 82 (2010) 205301, <http://dx.doi.org/10.1103/PhysRevB.82.205301>.
- [36] M. Levin, B.I. Halperin, B. Rosenow, Particle-Hole symmetry and the Pfaffian state, Phys. Rev. Lett. 99 (2007) 236806, <http://dx.doi.org/10.1103/PhysRevLett.99.236806>.
- [37] S.-S. Lee, S. Ryu, C. Nayak, M.P.A. Fisher, Particle-Hole symmetry and the $\nu = 5/2$ quantum Hall state, Phys. Rev. Lett. 99 (2007) 236807, <http://dx.doi.org/10.1103/PhysRevLett.99.236807>.
- [38] B.I. Halperin, Theory of the quantized Hall conductance, Helv. Phys. Acta 56 (1983) 75.
- [39] B.J. Overbosch, X.-G. Wen, Phase transitions on the edge of the $\nu = 5/2$ Pfaffian and anti-Pfaffian quantum Hall state, arXiv:0804.2087.
- [40] A. Cappelli, L.S. Georgiev, I.T. Todorov, A unified conformal field theory approach to paired quantum Hall states, Commun. Math. Phys. 205 (1999) 657–689, arXiv:preprint ESI-621 (1998); arXiv:hep-th/9810105.
- [41] M. Turek, K. Matveev, Cotunneling thermopower of single electron transistors, Phys. Rev. B 65 (2002) 115332.
- [42] M. Turek, J. Siewert, K. Richter, Thermopower of a superconducting single-electron transistor, Phys. Rev. B 71 (2005) 220503, <http://dx.doi.org/10.1103/PhysRevB.71.220503>.
- [43] C.L. Kane, M.P.A. Fisher, J. Polchinski, Randomness at the edge: theory of quantum Hall transport at filling $\nu = 2/3$, Phys. Rev. Lett. 72 (1994) 4129–4132, <http://dx.doi.org/10.1103/PhysRevLett.72.4129>.
- [44] C.L. Kane, M.P.A. Fisher, Contacts and edge-state equilibration in the fractional quantum hall effect, Phys. Rev. B 52 (1995) 17393–17405, <http://dx.doi.org/10.1103/PhysRevB.52.17393>.
- [45] A. Bid, N. Ofek, H. Inoue, M. Heiblum, C.L. Kane, V. Umansky, D. Mahalu, Observation of neutral modes in the fractional quantum Hall regime, Nature (London) 466 (2010) 585.
- [46] G. Yang, D.E. Feldman, Experimental constraints and a possible quantum Hall state at $\nu = 5/2$, arXiv:1406.2263.
- [47] S. Viefers, P. Koskinen, P.S. Deo, M. Manninen, Quantum rings for beginners: energy spectra and persistent currents, Physica E, Low-Dimens. Syst. Nanostruct. 21 (1) (2004) 1–35, <http://dx.doi.org/10.1016/j.physe.2003.08.076>, arXiv:cond-mat/0310064.
- [48] R.B. Laughlin, Anomalous quantum Hall effect: an incompressible quantum fluid with fractionally charged excitations, Phys. Rev. Lett. 50 (1983) 1395–1398, <http://dx.doi.org/10.1103/PhysRevLett.50.1395>.
- [49] J. Fröhlich, U.M. Studer, E. Thiran, A classification of quantum Hall fluids, J. Stat. Phys. 86 (1997) 821, arXiv:cond-mat/9503113.
- [50] J. Fröhlich, B. Pedrini, C. Schweigert, J. Walcher, Universality in quantum Hall systems: coset construction of incompressible states, J. Stat. Phys. 103 (2001) 527, arXiv:cond-mat/0002330.